EUROPEAN ORGANIZATION FOR NUCLEAR RESEARCH

Measurement of Triple Gauge-boson Couplings at 172 GeV

The ALEPH Collaboration

Abstract

Using data taken at 172 GeV by the ALEPH detector during 1996 corresponding to an integrated luminosity of 10.65 pb^{-1}, 34 semileptonically and 54 hadronically decaying $\mathrm{W}^{+}\mathrm{W}^{-}$ candidate events were found. The triple gauge-boson couplings, $\alpha_{\mathrm{w}\phi}$, α_{w} and $\alpha_{\mathrm{b}\phi}$, have been measured using Optimal Observables constructed from the kinematical information. The results are in agreement with the Standard Model expectation.

(Submitted to the 1997 lepton-photon conference, Hamburg)

1 Introduction

All evidence for the existence of triple gauge-boson vertices and measurements of the Triple Gauge-boson Couplings (TGC) has, until now, been indirect or is based on estimates from high energy $\mathrm{p\bar{p}}$ colliders [1].

The start of LEP2 at energies above the threshold for W pair production has allowed for the first time ever to study the fundamental non-Abelian gauge structure of the electroweak Standard Model directly in the very clean environment of $\mathrm{e^+e^-}$ collisions.

The present analysis uses a data sample with $\mathrm{e^+e^-} \to \mathrm{W^+W^-} \to e\nu q\bar{q}$, $\mu\nu q\bar{q}$, $q\bar{q}q\bar{q}$ candidate events recorded with the ALEPH detector at 172 GeV corresponding to a luminosity of 10.65 pb^{-1} to constrain models for the TGCs and thereby the underlying structure of the $\mathrm{Z^0W^+W^-}$ and $\gamma\mathrm{W^+W^-}$ vertices directly. The semileptonic channel $\tau\nu q\bar{q}$ and the fully leptonic channel $\ell\nu\ell\nu$ were not used in the analysis, because of their complicated kinematic reconstruction. A detailed description of the ALEPH detector and its performance can be found in Ref. [2] and [3].

The models studied here were introduced during the LEP2 workshop [4] and are referred to as the W_ϕ, W and B_ϕ models, respectively, with corresponding couplings $\alpha_{\mathrm{w}\phi}$, α_{w} and $\alpha_{\mathrm{b}\phi}$.

2 Triple Gauge-boson Couplings

Assuming the most general Gauge structure of the Electroweak Standard Model (SM) consistent with Lorentz invariance and $\mathrm{U(1)}_{EM}$ gauge invariance the $\mathrm{Z^0W^+W^-}$ and $\gamma\mathrm{W^+W^-}$ vertices can be comprehensively described by 14 independent couplings [5], 7 for each vertex, which – in the sense of a Taylor expansion – form a complete set [4].

Any theory incorporating new physics beyond the SM, while at the same time including the electroweak theory as an effective low-energy limit, may introduce small deviations in some of the general TGCs from their SM values. In this way precise measurements of the TGCs will not only establish a stringent test of the SM, but also probe for new physics in the bosonic sector. Virtual contributions within the SM also give non-standard contributions to the couplings of $\mathcal{O}(0.001)$ compatible to the effects from, for instance, SUSY theories [6].

The TGCs naturally split in three classes. Three TGCs, which conserve C and P individually, one TGC that violates C and P but is CP conserving and the remaining three TGCs describe CP violation in the triple gauge-boson sector. At present the large number of parameters does not allow an independent determination of all TGCs. However, based on very general theoretical considerations it is foreseen to be very unlikely to observe C-, P- or CP-violation at LEP2 [7, 8, 9]. Assuming electromagnetic gauge invariance and concentrating on the C- and P-conserving couplings reduces the number of TGCs to five: g_1^{Z}, κ_γ, κ_Z, λ_γ and λ_Z. The couplings related to the $\gamma\mathrm{W^+W^-}$ vertex determine properties of the W, such as the charge Q_{W}, the magnetic dipole moment μ_{W} and the electric quadrupole moment q_{W} of the W, via

$$\begin{aligned} Q_{\rm W} &= e g_1^\gamma \\ \mu_{\rm W} &= \frac{e}{2{\rm M_W}}(g_1^\gamma + \kappa_\gamma + \lambda_\gamma) \\ q_{\rm W} &= -\frac{e}{{\rm M_W^2}}(\kappa_\gamma - \lambda_\gamma). \end{aligned} \tag{1}$$

In the literature the TGCs are often referred to as anomalous couplings due to their connection with the magnetic moment.

Furthermore, the TGCs contribute, via loop corrections, to observables which can be measured at LEP1 and there has been a rich discussion on the bounds in the parameter space that can be deduced from the huge amount of LEP1 precision data [7, 10]. To parameterise the so-called "blind directions" in the multidimensional space of TGCs where the constraints from LEP1 analyses are very weak, three linear combination of these couplings have been proposed [4, 8, 5].

The three TGCs, $\alpha_{\rm w\phi}$, $\alpha_{\rm w}$ and $\alpha_{\rm b\phi}$, introduced to parameterise these linear combinations form the most general set of TGCs which can be embedded into an theory that preserves local $\mathrm{SU}(2)_L\times\mathrm{U}(1)_Y$ invariance. Such a requirement results in less violent divergences for observables relevant at LEP1. In terms of the notation in [4] they are

$$\begin{aligned} \alpha_{\rm w\phi} &= \Delta{\rm g}_1^{\rm Z}\cos^2\theta_{\rm W} \\ \alpha_{\rm w} &= \lambda_\gamma \\ \alpha_{\rm b\phi} &= \Delta\kappa_\gamma - \Delta{\rm g}_1^{\rm Z}\cos^2\theta_{\rm W}, \end{aligned} \tag{2}$$

along with constraints $\Delta\kappa_Z = \Delta{\rm g}_1^{\rm Z} - \Delta\kappa_\gamma\tan^2\theta_{\rm W}$ and $\lambda_\gamma = \lambda_Z$. The Δ denotes the deviations of the respective quantity from its non-zero SM value and $\theta_{\rm W}$ is the weak mixing angle.

In this analysis the couplings $\alpha_{\rm w\phi}$, $\alpha_{\rm w}$ and $\alpha_{\rm b\phi}$ are measured individually assuming the two other couplings to be fixed at zero, their SM expectation.

3 Event samples and selection

3.1 Monte Carlo samples

Several fully simulated Monte Carlo (MC) event samples have been used in the analysis. The main reference MC sample (50000 events) is obtained using the KORALW[11] generator where all the TGCs are set to their SM values. In addition, MC samples with 10000 events were generated with EXCALIBUR[12] and PYTHIA[13] for systematic studies. The KORALW and EXCALIBUR samples were generated with the full set of four-fermion diagrams contributing to $\mathrm{W^+W^-}$ final states, whereas PYTHIA only provides the $\mathrm{W^+W^-}$ diagrams. The cross-sections from KORALW and EXCALIBUR are in excellent agreement. Also, KORALW samples generated with different W masses around the current world-average, $\mathrm{M_W} = 80.356 \pm 0.125$ GeV/c^2 [14], have been used.

Furthermore, MC samples, each with 10000 events , were generated with non standard anomalous TGCs in order to check the reconstruction and fitting method.

These samples contain only the lowest order diagrams for W^+W^- pair production, the so-called CC03 [4] diagrams.

To check for possible systematic effects arising from colour reconnection a sample with colour reconnection was generated using EXCALIBUR. The model for colour reconnection assumed that strings are cylindrical space-time tubes and the reconnection probability is proportional to the space-time overlap of the string-systems from the two W-systems [15].

To estimate the effects from various background processes, PYTHIA was used to generate QCD and ZZ samples. In the ZZ sample, only events with final states not interfering with W^+W^- final states were used. Two photon ($\gamma\gamma$) processes were simulated the PHOT02 [16] generator. The corresponding integrated luminosity of each background sample was least 10 times as large as that of the data.

Finally the HERWIG[17] generator was used to generate a QCD sample, with the same luminosity as the PYTHIA QCD sample, for systematic studies of possible fragmentation and shape dependency of the QCD background.

3.2 Event selection

In this analysis all events were required to have at least five good tracks and a total charged energy greater than $0.12\sqrt{s}$ in order to discard low multiplicity background events.

3.2.1 Semileptonic channel

To reduce the QCD and two photon background a loose preselection was applied using the missing four-momentum.

The lepton identification was based on loose electron and muon identification criteria using standard ALEPH methods [3]. The reconstruction of electrons incorporates final-state-radiation and Bremsstrahlung in inactive material, taking into account the expected distribution of the radiation and the geometry of the ALEPH detector [18].

After preselection the events were passed to a neural network designed to select semileptonic events on lepton track basis with global event information. The most important quantities are topological variables, like, charged energy in a 10 degree cone around the lepton candidate, angle between the candidate track and the nearest charged track, and the missing energy direction. Also used is the measured missing four-momentum assumed to be carried by the neutrino and information about the lepton candidate energy.

Events with a neural network output smaller than 0.95 were rejected. The resulting efficiency was found to be 86% with a purity of 94% . The remaining part of the events were forced into two jets using the DURHAM (P-scheme) jet algorithm [19], disregarding the candidate for the lepton originating from one of the W bosons. Finally, the energies of the two jets were required to be greater than 10 GeV. After these requirements 34 semileptonic events, 14 $e\nu q\bar{q}$ and 20 $\mu\nu q\bar{q}$, were selected from data, with an expected background of 1.79 ± 0.06. The event selection and

Channel	Semileptonic	Hadronic
data	34	54
	Normalised to $\mathcal{L} = 10.65$ pb^{-1}	
W$^+$W$^-$ MC signal	32.10	45.90
W$^+$W$^-$ MC non-signal	1.08	0.20
MC QCD	0.41	6.04
MC $\gamma\gamma$	0.21	0.00
MC ZZ	0.09	0.53
MC Total	33.9	52.6

Table 1: *The number of events after selection for data and MC simulation in the semileptonic and hadronic channel. For the MC simulation, the contributions from different types of processes are given separately.*

background contamination is summarised in Table 1. The main background, 1.08 events, comes from the semileptonic $\tau\nu q\bar{q}$ channel where the τ is misidentified.

3.2.2 Hadronic channel

At this stage the events are forced into four jets using the DURHAM (P scheme) jet algorithm and the resulting jets were required to have more than 10 GeV in order to reject events with large energy losses and badly reconstructed jets.

To extract the W$^+$W$^-$ signal with high purity and efficiency, the main selection is based on the output of a neural network. The neural network input consist of 21 variables which were chosen to optimise the selection efficiency. The neural net was trained on a WW MC signal sample and QCD, $\gamma\gamma$, ZZ, Zee, and $\tau^+\tau^-$ background samples. A description of the neural network can be found in [20]. For a cut of 0.5 on the neural network output the events are selected with an efficiency of 75% and a purity of 87% . In total 54 events passed the criteria with an expected background of 6.77 ± 0.30. The event selection and background contamination is given in Table 1.

4 Kinematic reconstruction

The important kinematic quantities for TGC measurements in W$^+$W$^-$ events are the five variables:

- $cos(\theta)$, the production angle of the W$^-$.
- $cos(\theta_{1,2})$, the polar decay angle of the charged lepton or down type quark with respect to the flight direction of the W$^{-,+}$, measured in its rest frame.
- $\phi_{1,2}$, the azimuthal decay angle of the charged lepton or down type quark with respect to the plane defined by the direction of W$^{-,+}$ and the incoming electron.

In the following a description of the reconstruction of the four-momenta of the W^+W^- decay products, which determine these angles, is presented.

4.1 Semileptonic events

In order to correct for the finite energy resolution of the detector combined with the loss of particles in the beam pipe or in cracks, the events are subjected to a kinematical fit using four-momenta conservation and reference mass constraints by requiring that the two decaying systems should be Gaussian distributed around the W mass. The resulting four-momenta of the four reconstructed objects are used in the determination of the TGCs. The effects of initial state radiation have not been accounted for in the kinematic fit, but this is taken into account in the final fitting procedure used to extract the TGCs. The resulting RMS of the resolution for the cosine of the W^- production angle for semileptonic events was found to be 0.16.

For semileptonic events the charge of the reconstructed lepton determines the W^- direction and hence allows for unambiguous determination of the primary variable for measurement of the TGCs, the production angle. Likewise is the leptonically decaying W-system completely determined, but in case of the hadronically decaying W the flavour of the quarks has not been determined and it is necessary to fold over the two four-momentum configurations for that decay. The possibility to use flavour-tagging or jet-charge tagging to determine the flavour of the quarks has been studied, but with the present statistics the improvement of the bounds on TGCs was negligible. However, the unambiguous determination of the production angle results in a relatively high sensitivity to the TGCs in semileptonic events.

4.2 Hadronic events

For the hadronic W^+W^- events the reconstruction of the relevant information is more complicated since there is no clean signature of the W^- direction nor any information of the particle flavours in both W systems. In this case the four jets can be paired in three different ways. To select the best pairing the kinematic fitting procedure was applied to all three pairings. The four-momenta obtained in the kinematic fit for the pairing with the lowest χ^2 value were then used in the determination of the TGCs, while the other combinations are discarded. The efficiency of the pairing was found to be 84% . The resulting RMS of the resolution on the cosine of the W^- production angle for hadronic events was found to be 0.18.

To assign a jet pair to the W^+ or W^- a jet charge algorithm is used. The charge difference between the two W-systems is 2 leading to a relatively high separation efficiency. The jet charge is obtained from the pseudo-rapidity weighted charge of jet particles:

$$Q_{\mathrm{jet}} = \frac{\sum_i \eta_i Q_i}{\sum_i \eta_i} \tag{3}$$

where the sum runs over all particles assigned to the jet. The W charge is then defined by the sum of the two jets assigned to the W, $Q_{\mathrm{W}} = Q_{\mathrm{jet}1} + Q_{\mathrm{jet}2}$. A W charge is then assigned to the jet pair based on the difference to the W^+ with a probability P_+. The probability P_+ is obtained as

$$P_+ = \frac{N_+(Q_{\mathrm{W1}} - Q_{\mathrm{W2}})}{N_+(Q_{\mathrm{W1}} - Q_{\mathrm{W2}}) + N_+(-Q_{\mathrm{W1}} + Q_{\mathrm{W2}})}, \tag{4}$$

where N_+ is the probability distribution for true W^+ decays obtained from MC samples. Figure 1a shows the probability distribution for true W^+ and W^- decays. The distribution of P_+, obtained from MC simulation, is depicted in Fig. 1b. The distribution of $Q_{\mathrm{W1}} - Q_{\mathrm{W2}}$ for $P_+ < 0.5$ ($P_+ > 0.5$) is shown in Fig. 1c(d). The data is well reproduced by the MC simulation. The charge assignment efficiency for correctly paired hadronic $\mathrm{W}^+\mathrm{W}^-$ events amounts to approximately 80% for a cut on $P_+ > 0.5$.

The quark flavours are not determined which leads to a two fold ambiguity per W. Considering the W charge as undetermined implies that there is an eight fold ambiguity per hadronic event.

5 Measurement of the TGCs

Several methods to extract the anomalous couplings have been investigated in order to evaluate their sensitivity to the TGCs and study their advantages and drawbacks.

One method is a maximum log-likelihood fit where the event probability is evaluated from the differential cross section using the measured kinematical variables. The primary advantage of this method is that it exploits the full angular information available and should thus provide maximum sensitivity to the TGCs. However, the likelihood includes neither background nor experimental effects which consequently leads to the need of a bias correction and calibration of errors. Figure 2a shows the calibration curve for α_{w} in the semileptonic channel. The curve was obtained from fits to several MC samples corresponding to the luminosity of the data including statistical fluctuations. The curve illustrates the non-linear behaviour of this method, leading to a degradation in resolution.

A canonical way to account for detector smearing and acceptance is to determine the couplings by a standard five dimensional binned likelihood fit using MC simulation. However, to bin the relevant kinematical information according to the experimental resolution, would lead to a practically unacceptable amount of bins.

Fits to the measured $\cos(\theta_{\mathrm{W}})$ distribution avoids the above difficulties, but looses a considerable amount of information, especially for the semileptonic channel where the leptonic quantities give important information on the W helicity.

Instead the dimensionality can be reduced by introducing the so-called 'Optimal Observables' (OO) which project the relevant kinematical information sensitive to a certain TGC onto a one dimensional distribution [22]. The OO for a given TGC, α_i, is defined as the derivative of the differential cross section with respect to the coupling evaluated at the SM value

$$OO_i = \frac{1}{d\tilde{\sigma}|_{\alpha_i=0(\mathrm{SM})}} \frac{d}{d\alpha_i}(d\tilde{\sigma}(\alpha_i)), \tag{5}$$

where $d\tilde{\sigma}(\Omega, \overline{\alpha})$ denotes the differential cross section after folding over ambiguities, i.e.

$$d\tilde{\sigma}(\Omega, \overline{\alpha})_{\ell\nu q\bar{q}} = \left[\frac{d\sigma}{d\Omega_{\ell\nu j_1 j_2}} + \frac{d\sigma}{d\Omega_{\ell\nu j_2 j_1}}\right] \tag{6}$$

in the semileptonic case where the two fold ambiguity from the hadronically decaying W is summed. In the hadronic case a summation is performed over the eight fold ambiguity, each weighted with the appropriate charge probability.

For each detected event OO_i is calculated and a likelihood fit is performed to the distribution of an Optimal Observable using

$$\ln \mathcal{L} = \sum_{i=1}^{N} \ln P(OO_i, \overline{\alpha}), \tag{7}$$

where the probability, $P(OO_i, \overline{\alpha})$, is evaluated from the distribution of OO_i, obtained from MC simulation. The probability can be constructed for different values of the TGCs by reweighting the MC events.

The total number of events observed is included by adding a Poisson term to the likelihood function [21].

By construction, this method is bias free and takes into account any experimental effects, provided that the MC simulation describes data. The linear behaviour of this method is shown in Fig. 2b where the "calibration curve" for α_{w} is shown.

5.1 Results

In this section the results for the three TGCs, $\alpha_{\mathrm{w}\phi}$, α_{w} and $\alpha_{\mathrm{b}\phi}$, are presented for fits using the semileptonic and hadronic $\mathrm{W}^+\mathrm{W}^-$ channels and combined fits. All the fits have been made using the current world average of the W mass, 80.356 ± 0.125 GeV$/c^2$, a LEP energy of $\mathrm{E}_{LEP} = 172.086 \pm 0.060$ GeV [23] and an integrated luminosity of 10.65 ± 0.08 pb^{-1}.

While the main sensitivity to the TGCs stems from the kinematical distributions the total number of observed events provides straightforward bounds. Figure 3 shows the total number of expected events, normalised to the luminosity, as function of $\alpha_{\mathrm{w}\phi}$, α_{w} and $\alpha_{\mathrm{b}\phi}$. The total number of selected events, hadronic and semileptonic, in the data (88) is also indicated in this figure. The distributions of $\cos\theta$ for semileptonic and hadronic events are shown Fig. 4. The data is well reproduced by the SM MC simulation.

Results for $\alpha_{\mathrm{w}\phi}$, α_{w} and $\alpha_{\mathrm{b}\phi}$ from semileptonic and hadronic events using the fits to the Optimal Observables are listed in Table 3. The distributions of the Optimal Observables can be found in Fig. 5. The MC distributions for different values of the couplings are also shown, illustrating the sensitivity to the TGCs.

The combined results from the analyses of the semileptonic and hadronic channels have been extracted by fits to the sum of the log-likelihood curves from the individual channels. The resulting negative $2\ln\mathcal{L}$ distributions are shown in Fig. 6 for the three TGCs. The results from the fits are summarised in Table 3.

6 Systematic uncertainties

The systematic uncertainties were, wherever possible, determined by modifying the MC simulation for the effect under study. In some cases it was necessary to repeat the event reconstruction, after modification, for both data and MC simulation. Unavoidably, the systematic uncertainties estimated in this way will be sensitive to statistical effects and therefore overestimated.

In the following several sources of systematic errors and their determination are briefly described.

- The analysis was repeated using MC samples generated at different values of $\mathrm{M_W}$ to investigate the effects due to the uncertainty in the W mass, $\mathrm{M_W} = 80.356 \pm 0.125$ GeV. The values of the the measured couplings changed by typically 10% of the statistical uncertainties in the combined fits.

- The LEP energy is used in the kinematical fitting procedure, where it enters via the constrain of four momenta conservation. Its value was varied in the range $\mathrm{E}_{LEP} = 172.086 \pm 0.060$ GeV, which had negligible effect on the results.

- To check for possible deviation of the calorimetric energy measurement between data and MC simulation, the hadronic part of the measured energy was varied by 4% in the MC simulation (denoted HAC). Independently, the electromagnetic component was varied by 1.5% (denoted EMC). These variations are based on detailed comparisons between data and MC simulation. The results changed by approximately by 5% of the statistical uncertainties in the combined fits.

- The background from QCD was changed by 5%, based on comparisons between data and MC simulation. We repeated the analysis using the HERWIG QCD generator, which uses a different hadronisation model, to account for possible shape and fragmentation dependence in the main background. The effects on the results are below 3% of the statistical uncertainties in the combined fits.

- The background from $\gamma\gamma$ and ZZ events was varied by 30% which resulted in negligible changes on the measured couplings.

- To investigate the effects due to the uncertainties from fragmentation and jet reconstruction, the following checks were performed.

  – The standard DURHAM (P-scheme) algorithm was replaced by DURHAM (E-scheme) and JADE [24] (P-scheme) in both data and MC simulation. The DURHAM and JADE algorithms represent two conceptually different criteria for forming jets, transverse momentum versus invariant mass, respectively, which is affected differently by fragmentation. This resulted in considerable changes on the measured couplings in the hadronic channel, about 60% of the statistical uncertainty. The changes in the semileptonic channel and for combined result were typically 20% of the statistical uncertainty.

Source	$\alpha_{w\phi}$	α_w	$\alpha_{b\phi}$
Mw	$-0.02/-0.04$	$+0.04/+0.02$	± 0.03
LEP Energy	–	–	–
HAC ($\pm 4\%$)	± 0.01	± 0.02	± 0.02
EMC ($\pm 1.5\%$)	–	± 0.03	± 0.02
HERWIG QCD MC	-0.01	-0.01	–
QCD ($\pm 5\%$)	–	–	–
$\gamma\gamma$ MC ($\pm 30\%$)	–	–	–
EXCALIBUR MC	0.06	0.04	-0.24
MC statistics	± 0.01	± 0.02	± 0.05
Colour reconnection	-0.10	-0.01	0.10
PYTHIA MC	-0.02	-0.09	-0.21
JADE p	$+0.06$	-0.16	0.25
DURHAM E	$+0.06$	0.09	0.08
Jet-charge	± 0.015	± 0.036	± 0.02
Total	$+0.11/-0.12$	$+0.12/-0.19$	$+0.29/-0.33$

Table 2: *Summary of systematic uncertainties for $\alpha_{w\phi}$, α_w and $\alpha_{b\phi}$, for the combined fits. A description of the different sources is given in the text.*

  - For the hadronic channel, we repeated the analysis for the EXCALIBUR MC simulation with and without colour reconnection. The effect on the couplings was considerable for $\alpha_{w\phi}$ where it amounted to approximately 40% of the statistical uncertainties in the combined fit.
  - To check the effects from the uncertainties of the jet charge we shifted the reconstructed W charge by 0.01. This number is based on comparisons between data and MC simulation (Z peak data). The changes in the couplings was about 6% of the statistical uncertainties in the combined fits.

- Radiative corrections.
  The analysis was repeated using events generated with the PYTHIA generator, which uses a different model to implement the radiative corrections. The values of the couplings changed by 10% of their statistical uncertainties. Furthermore we used the EXCALIBUR MC sample, which has collinear initial state radiation [25], in contrast to KORALW and PYTHIA. The effect on the couplings was below 20% of the statistical uncertainties in the combined fits, highest for $\alpha_{w\phi}$.

- The uncertainty due to the use of a finite number of MC events was evaluated and found to be less than 4% of the statistical uncertainties in the combined fits.

The results are graphically displayed in Fig. 7 for the combined fits. The shaded bands in these figures represent the statistical uncertainties.

The results for the combined fits are summarised in Table 2.

Optimal Observable		
Hadronic	semileptonic	Combined
$\alpha_{\mathrm{w}\phi} = -0.29^{+0.30(0.07)}_{-0.28(0.10)}$	$\alpha_{\mathrm{w}\phi} = 0.38^{+0.41(0.14)}_{-0.53(0.22)}$	$\alpha_{\mathrm{w}\phi} = -0.14^{+0.27(0.11)}_{-0.25(0.12)}$
$\alpha_{\mathrm{w}} = -0.31^{+0.60(0.15)}_{-0.53(0.10)}$	$\alpha_{\mathrm{w}} = 0.96^{+0.58(0.38)}_{-0.85(0.86)}$	$\alpha_{\mathrm{w}} = 0.06^{+0.58(0.12)}_{-0.52(0.19)}$
$\alpha_{\mathrm{b}\phi} = -1.19^{+3.06(0.51)}_{-0.77(0.56)}$	$\alpha_{\mathrm{b}\phi} = 0.94^{+1.37(0.29)}_{-1.55(0.45)}$	$\alpha_{\mathrm{b}\phi} = 1.01^{+0.86(0.29)}_{-2.14(0.33)}$

Table 3: *The final results for $\alpha_{\mathrm{w}\phi}$, α_{w} and $\alpha_{\mathrm{b}\phi}$, respectively, for fits to the semileptonic and hadronic channels and the combined fit. The systematic uncertainties are shown in brackets.*

The individual systematic effects are combined in quadrature, separately for positive and negative deviations from the standard values of the measured couplings. In the combined fits, the systematic uncertainties amount to 40% , 20% and 20% of the statistical uncertainties for $\alpha_{\mathrm{w}\phi}$, α_{w} and $\alpha_{\mathrm{b}\phi}$, respectively.

6.1 Additional checks

All the fits used in this study rely on the applicability of MC event reweighting. The validity of the reweighting procedure was checked by repeating the fits using MC samples *generated* with non-zero values for the TGCs. In all cases the results were in agreement within the statistical uncertainty of the MC samples. Furthermore, the reweighting procedure has been performed with both four-fermion and CC03 matrix-elements as a cross check and to see the impact of non-CC03 diagrams.

To check the stability and the possible biases of the fitting procedure, fits were performed to several MC samples as already mentioned in section 5. These samples, typically 200, were then reweighted to non-zero values for the TGCs and passed through the analysis chain. The resulting distributions of the fit values show good correspondence with the confidence intervals obtained for data.

Finally, the stability of the analysis with respect to the event selection was tested by varying the main selection criteria within reasonable limits. The effects of all these additional checks were well below the total systematic uncertainties.

6.2 Final results

The final results for fits to the semileptonic and hadronic channels and the combined fit are summarised for $\alpha_{\mathrm{w}\phi}$, α_{w} and $\alpha_{\mathrm{b}\phi}$, respectively, in Table 3. The corresponding 95% confidence levels have been obtained as the point of interception with $\Delta(-2\ln\mathcal{L}) = 3.84$ yielding

$$\begin{aligned} -0.62(0.14) &< \alpha_{\mathrm{w}\phi} < 0.41(0.12) \\ -0.89(0.20) &< \alpha_{\mathrm{w}} < 1.17(0.15) \\ -1.92(0.34) &< \alpha_{\mathrm{b}\phi} < 2.56(0.31). \end{aligned}$$

The systematic uncertainties for the 95% confidence intervals were estimated by scaling the effects. For the effects of jet algorithms or MC generators this procedure is not possible and the induced deviations were used.

7 Summary and conclusion

A measurement of Triple Gauge-boson Couplings is presented in the semileptonic, $e\nu q\bar{q}$ and $\mu\nu q\bar{q}$, and hadronic decay modes in W pair production, using a data sample collected by the ALEPH detector at a centre of mass energy of 172.086 GeV, corresponding to an integrated luminosity of 10.65 pb^{-1}.

The analysis includes full kinematic information and accounts for detector effects and background. The Triple Gauge-boson Couplings are extracted by using likelihood estimation based on one dimensional distributions of Optimal Observables, constructed from the four fermion differential cross section.

Single parameter fits to the combined semileptonic and hadronic analyses for the three models, W_ϕ, W and B_ϕ, yielded

$$\boxed{\begin{array}{lcrl} \alpha_{\mathrm{w}\phi} & = & -0.14^{+0.27(0.11)}_{-0.25(0.12)} & \text{assuming } \alpha_{\mathrm{w}} = \alpha_{\mathrm{b}\phi} = 0 \\ \alpha_{\mathrm{w}} & = & 0.06^{+0.58(0.12)}_{-0.52(0.19)} & \text{assuming } \alpha_{\mathrm{w}\phi} = \alpha_{\mathrm{b}\phi} = 0 \\ \alpha_{\mathrm{b}\phi} & = & 1.01^{+0.86(0.29)}_{-2.14(0.33)} & \text{assuming } \alpha_{\mathrm{w}\phi} = \alpha_{\mathrm{w}} = 0 \end{array}}$$

in excellent agreement with the Standard Model prediction. The separate results in both the hadronic and semileptonic channels are also consistent with the SM predictions. The corresponding 95% confidence levels are

$$\begin{array}{r} -0.62(0.14) < \alpha_{\mathrm{w}\phi} < 0.41(0.12) \\ -0.89(0.20) < \alpha_{\mathrm{w}} < 1.17(0.15) \\ -1.92(0.34) < \alpha_{\mathrm{b}\phi} < 2.56(0.31). \end{array}$$

The systematic uncertainties are dominated by the choice of the jet reconstruction algorithm and colour reconnection, followed by the effects of using different MC samples to check the hadronisation and radiative corrections. However, the uncertainties are still largely dominated by the statistical precision of the data samples.

8 Acknowledgements

It is a pleasure to thank the SL division of CERN for the excellent performance of the LEP collider. We would also like to express our appreciation of the work by all engineers and technicians in our institutions, providing the successful operation of ALEPH. Those of us from non-member countries thank CERN for its hospitality. We thank M. Skrzypek for providing a routine to evaluate the matrix element from KORALW.

References

[1] The CDF Collaboration, F. Abe *et al.*, *Phys. Rev. Lett.* **75** (1995) 1017.
The D0 Collaboration, S. Abachi *et al.*, *Phys. Rev. Lett.* **75** (1995) 1023, S. Abachi *et al.*, *Phys. Rev. Lett.* **77** (1996) 3303.

[2] ALEPH Collaboration, *Nucl. Instr. Meth.* **A 294** (1990) 121.

[3] ALEPH Collaboration, *Nucl. Instr. Meth.* **A 360** (1995) 481.

[4] G. Gounaris, J.-L. Kneur and D. Zeppenfeld, from "Physics at LEP2", CERN 96-01 p. 525, editors G. Altarelli, T. Sjöstrand and F. Zwirner.

[5] K. Hagiwara, R. Peccei, D. Zeppenfeld and K. Hikasa, *Nucl. Phys.* **B 282** (1987) 253.

[6] A. B. Lahanas and V. C. Spanos, *Phys. Lett.* **B 334** (1994) 378 HEP-PH/9504340;.E. N. Argyres, A. B. Lahanas, C. G. Papadopoulos and V. C. Spanos, UA/NPPS-18B (1995).
A. Arhrib, J.-L. Kneur and G. Moultaka, CERN-TH/95-344 (hep-ph/9512437).

[7] A. De Rújula, M.B. Gavela, O. Pène and F.J. Vegas, *Nucl. Phys.* **B357** (1991) 311.

[8] M. Bilenky, J.L. Kneur, F.M. Renard and D. Schildknecht, *Nucl. Phys.* **B409** (1993) 22.

[9] G. Gounaris, J. Layssac, G. Moultaka and F.M. Renard, *Int. J. Mod. Phys.* **A 8** (1993) 3285.

[10] A. De Rújula, M.B. Gavela, P. Hernandez and E. Massó, *Nucl. Phys.* **B384** (1992) 3.

[11] M. Skrzypek, S. Jadach, W. Placzek and Z. Was, *Computer Phys. Comm.* **94** (1996) 216.

[12] F.A. Berends, R. Pittau and R. Kleiss, *Nucl. Phys.* **B 424** (1994) 308.

[13] T. Sjöstrand, *Computer Phys. Comm.* **82** (1994) 74.

[14] The LEP Collaborations, the LEP Electroweak Working Group and the SLD Heavy Flavour Group. CERN-PPE/96-183.

[15] T. Sjöstrand and A.Khoze, *Phys. Rev.* **72** (1994) 28.

[16] ALEPH Collaboration, *Phys. Lett.* **B313** (1993) 509.

[17] G. Marchesini, B. R. Webber, G. Abbiendi, I. G. Knowles, M. H. Seymour and L. Stanco, *Computer Phys. Comm.* **67** (1992) 465.

[18] ALEPH Collaboration, *Phys. Lett.* **B 295** (1992) 396.

[19] Yu. L. Dokshitzer,*J. Phys. G.* **17** (1991) 1441.

[20] ALEPH Collaboration, EPS-HEP/97-600, to appear in the proceedings of EPS-HEP 1997.

[21] A.G. Frodesen, O. Skjeggestad and H. Tofte, "Probability and Statistics in Particle Physics" (Universitetsforlaget, Bergen 1978).

[22] M. Diehl and O. Nacthmann, *Zeit. Phys.* **C62** (1994) 397.

[23] Working group on LEP energy, private communication.

[24] JADE Collaboration, *Zeit. Phys.* **C33** (1986) 23 JADE.Colloaboration, *Phys. Lett.* **B213** (1988) 235.

[25] F.A. Berends, G. Burgers and W.L. Van Neerven, *Phys. Lett.* **B185** (1987) 395; *Nucl. Phys.* **B297** (1988) 429; *Nucl. Phys.* **B304** (1988) 921.

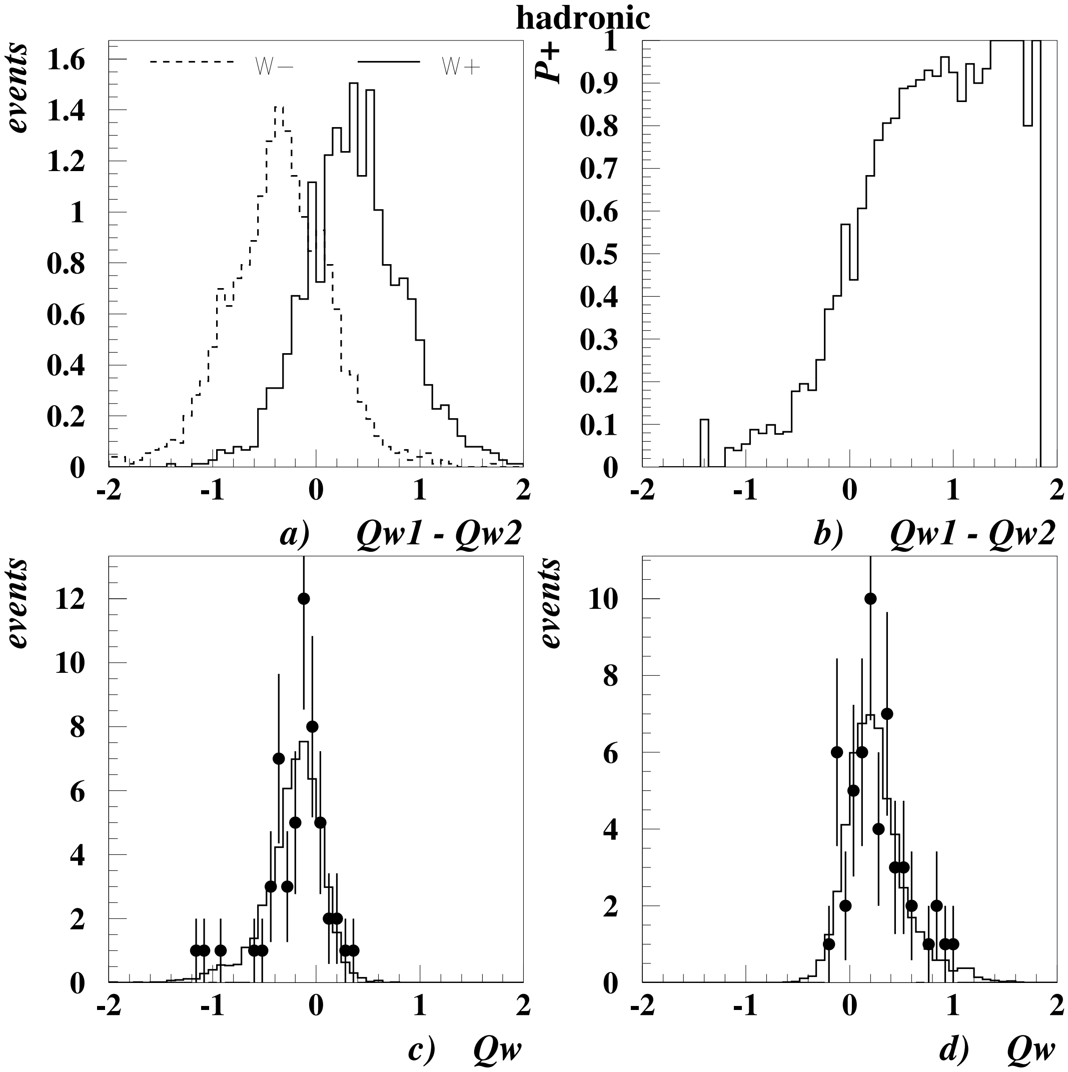

Figure 1: *W charge tagging distributions. a) The distribution of the charge difference for true W^+ decay (solid line) and true W^- (dashed line) for MC events as funtion of the charge difference between the two W's. b) The probability distribution, P_+, for a W^+ as function of the charge difference between the two W's. c) and d) Experimental distributions of W^- (selected by $P_+ < 0.5$) and W^+ (selected by $P_+ > 0.5$) reconstructed charges, respectively. The data are represented by the dots and the MC simulation by the histograms.*

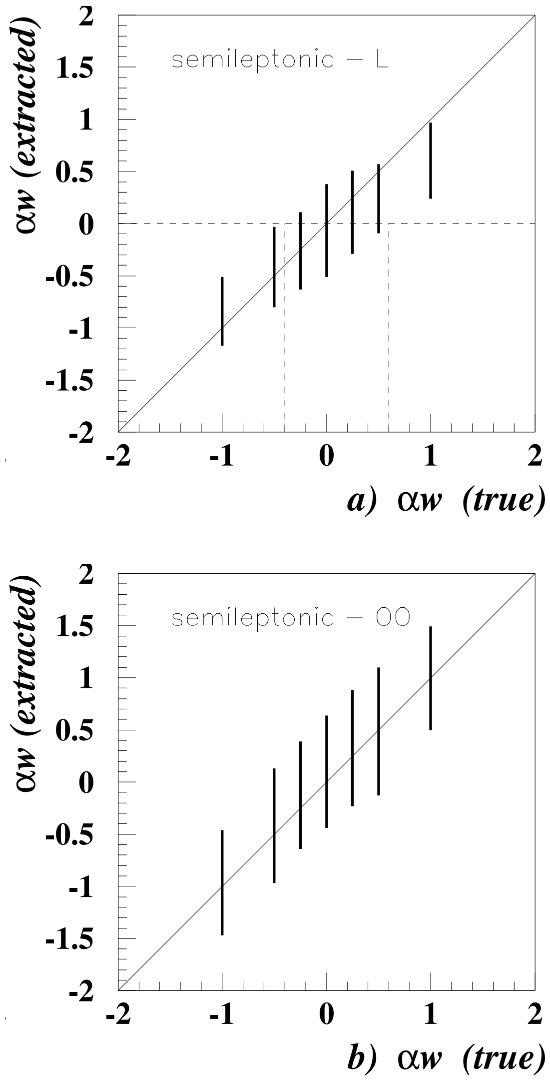

Figure 2: *The 68% confidence intervals for extracted values of $\alpha_{\rm w}$ versus $\alpha_{\rm w}$ true obtained from typical 200 pseudo experiments. a) The results for the semileptonic W events for straightforward likelihood fits. b) The results for the semileptonic W events for fits using the Optimal Observable.*

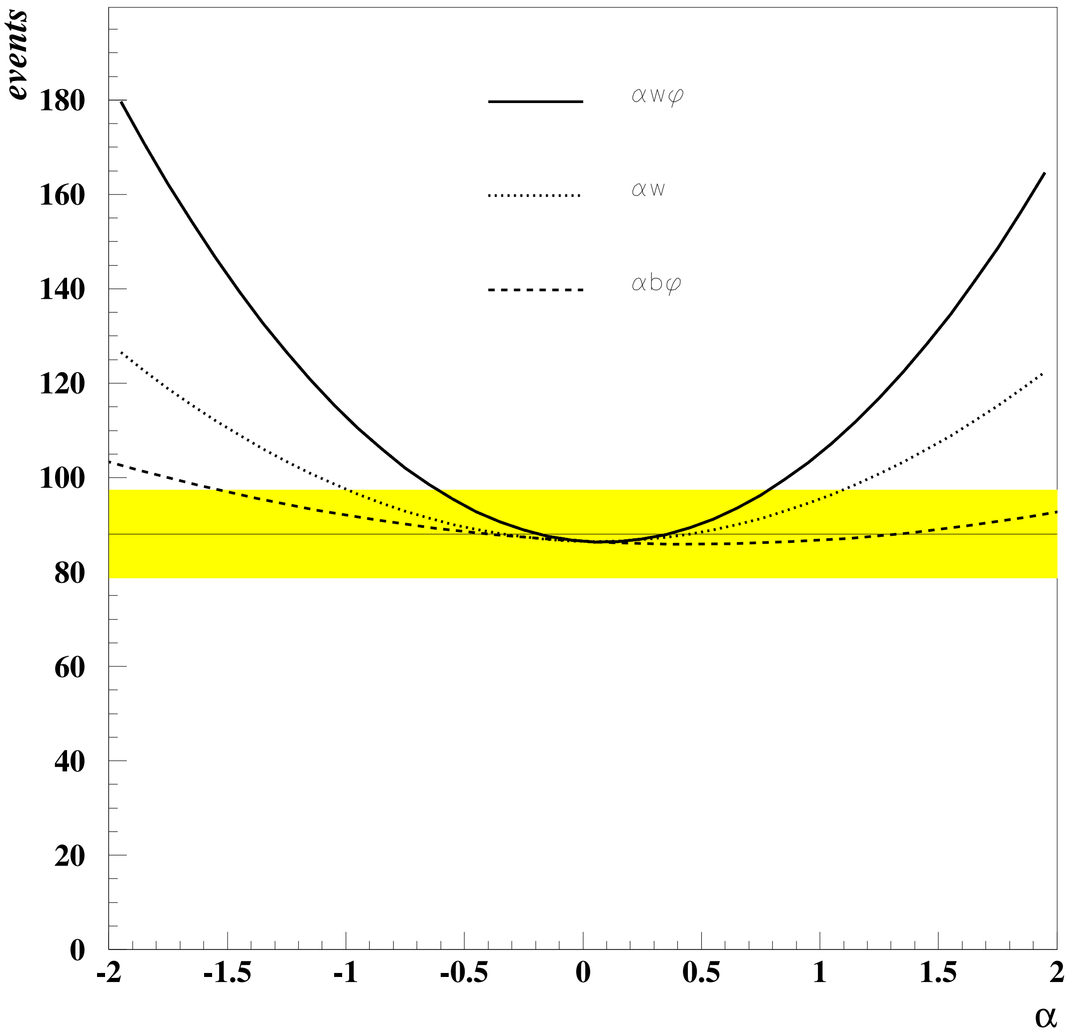

Figure 3: *The number of expected events as function of the couplings as indicated in the plot. The curve for each TGC is obtained under the assumption that the two other TGCs are fixed at zero, their Standard Model value. The total number of observed events, semileptonic and hadronic, is represented by the horizontal line and the corresponding statistical uncertainty is indicated by the band.*

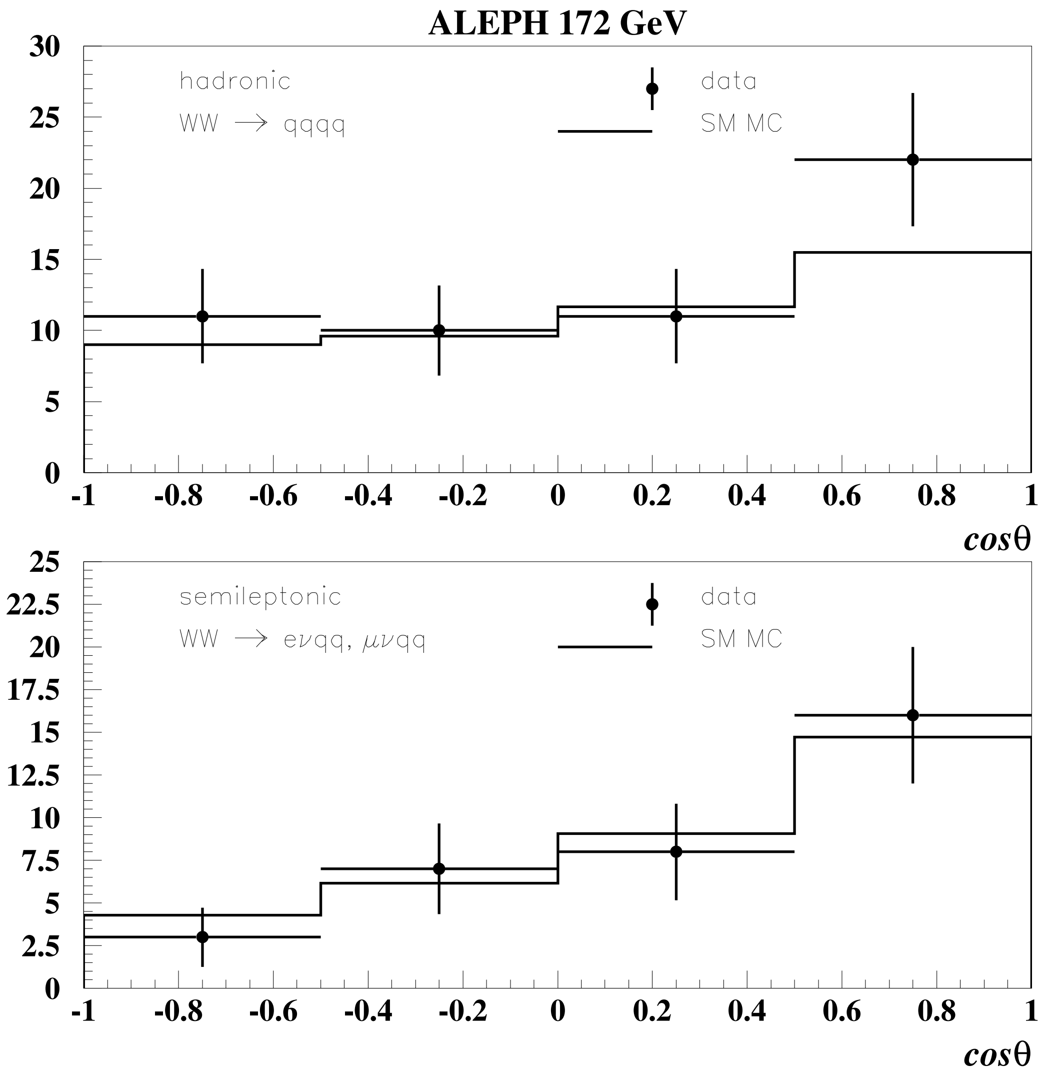

Figure 4: *The distribution of the production angle of the W^-, $cos(\theta)$, for hadronic and semileptonic channels. The data is represented by the solid dots and the MC simulation by the lines.*

ALEPH 172 GeV

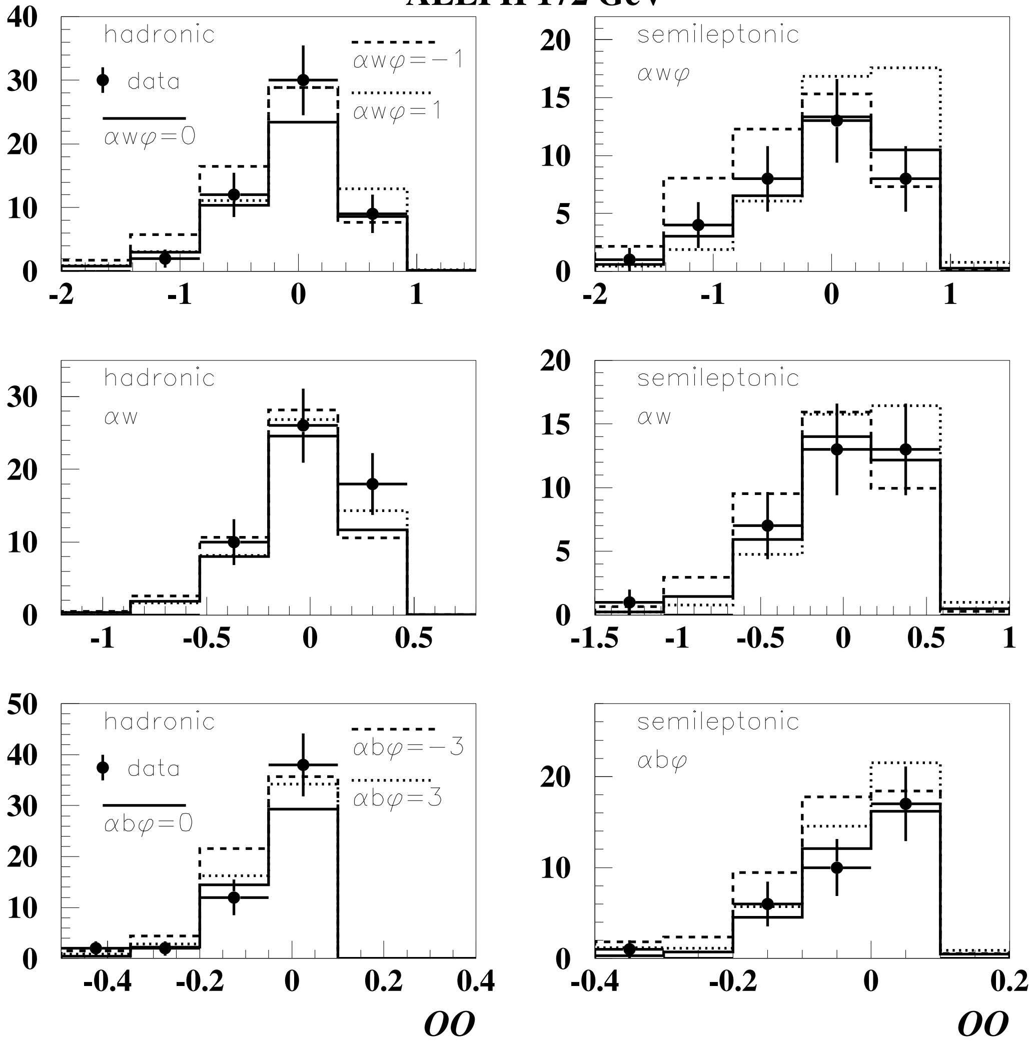

Figure 5: *The distribution of the Optimal Observable for various values of the couplings $\alpha_{\mathrm{w}\phi}$, α_{w} and $\alpha_{\mathrm{b}\phi}$ as indicated in the plots for hadronic and semileptonic channels. The data is represented by the solid dots and the MC simulation by the histograms. For the couplings $\alpha_{\mathrm{w}\phi}$ and α_{w} the solid histograms represent the Standard Model expectation, while the dashed and dotted histograms show the distributions for values of the couplings -1 and 1, respectively. The corresponding histograms for $\alpha_{\mathrm{b}\phi}$ represent values of $\alpha_{\mathrm{b}\phi} = -3$ and 3.*

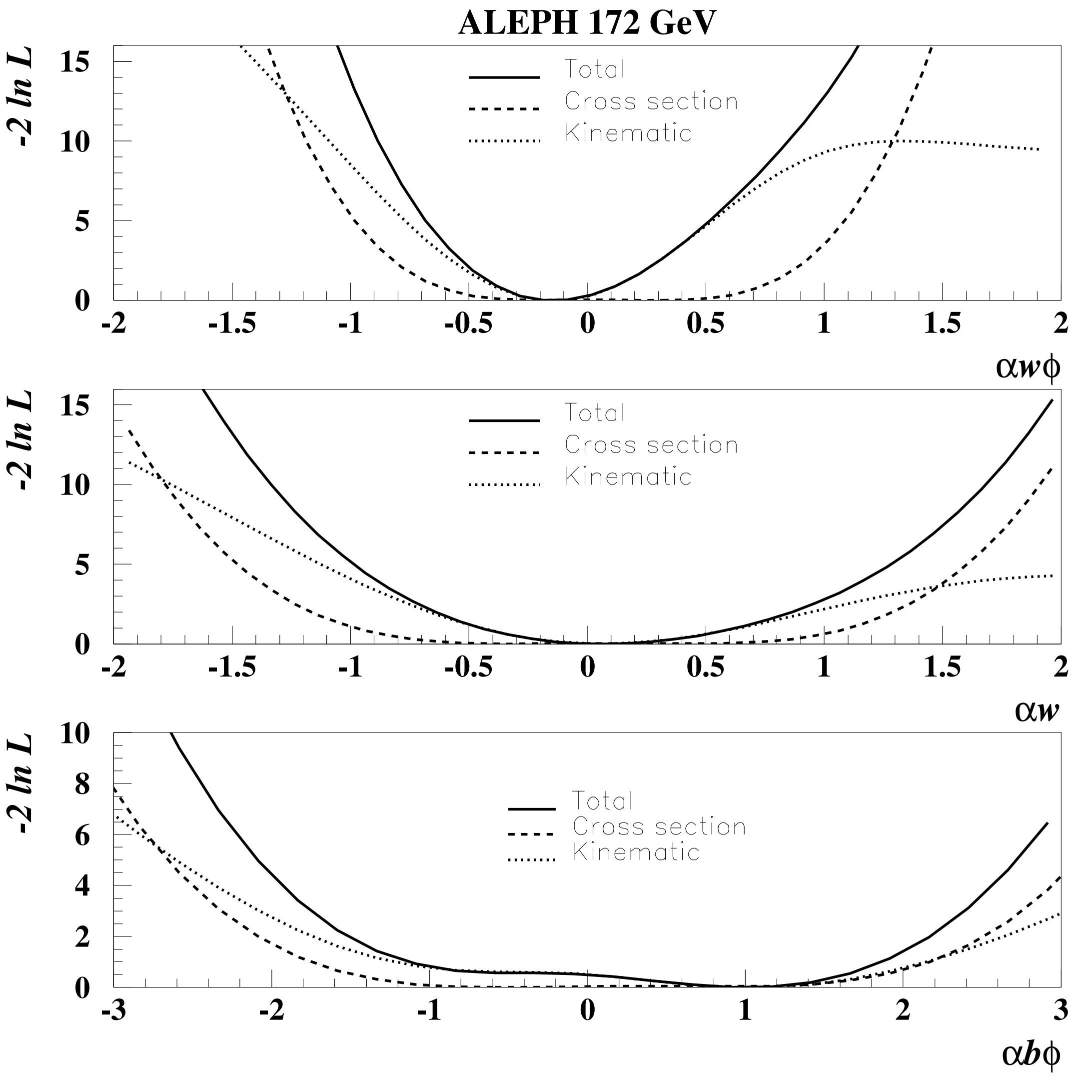

Figure 6: *The quantity $-2\ln\mathcal{L}$ for the combined fit to both semileptonic and hadronic channels for the three couplings $\alpha_{\mathrm{w}\phi}$, α_{w} and $\alpha_{\mathrm{b}\phi}$. The contribution of the cross section (dashed curve) and kinematic information (dotted curve) are also shown. Top: The curves for $\alpha_{\mathrm{w}\phi}$. Centre: The curves for α_{w}. Bottom: The curves for $\alpha_{\mathrm{b}\phi}$.*

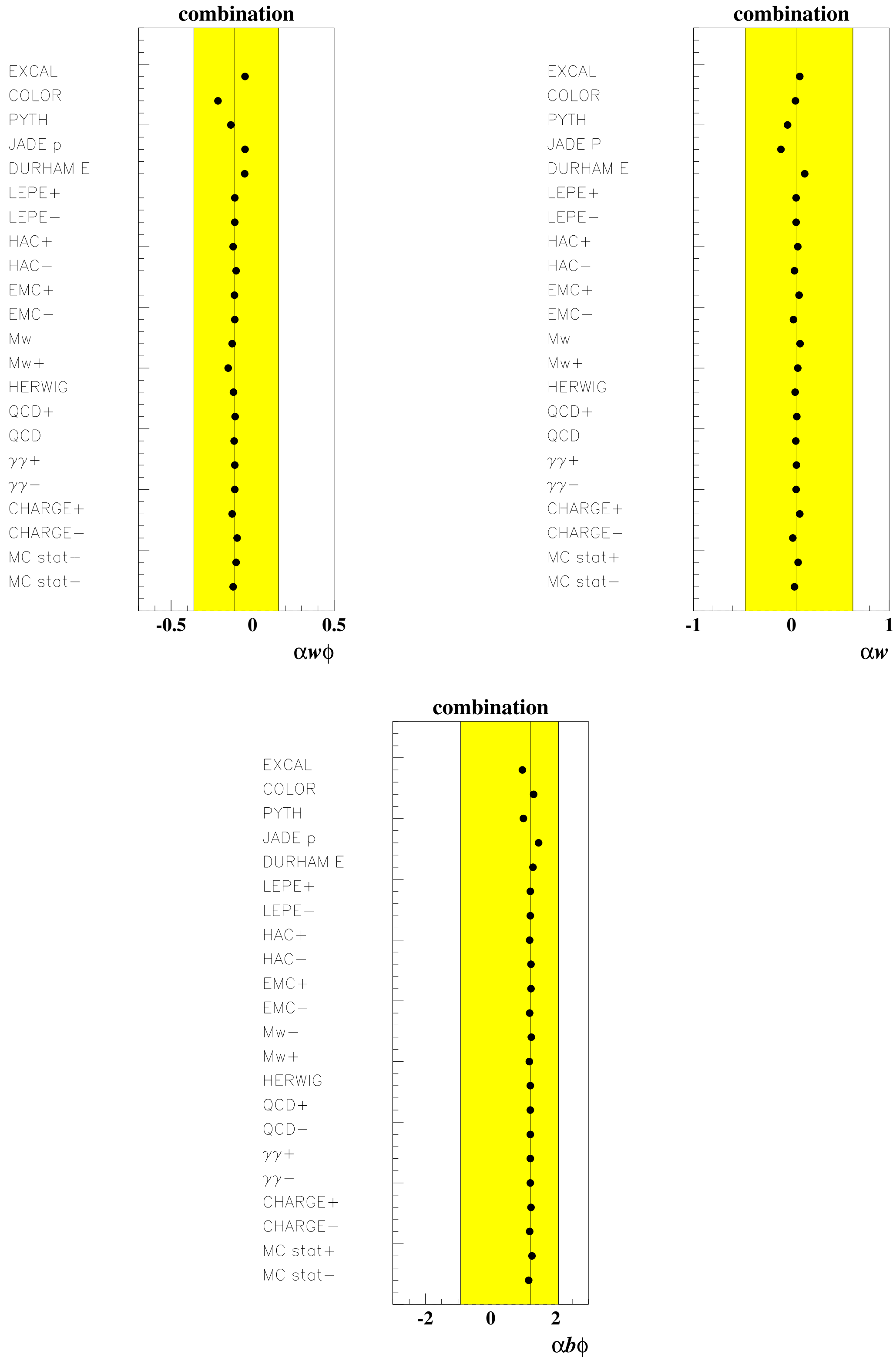

Figure 7: *The contribution of the individual systematic uncertainties compared with the statistical uncertainty, represented by shaded bands, are shown for $\alpha_{w\phi}$, α_{w} and $\alpha_{b\phi}$, respectively, for the combined fits using the semileptonic and hadronic channels.*